

PAPER • OPEN ACCESS

Influence of Deposited Material Energy on Superconducting Properties of the WSi Films

To cite this article: D D Vasilev *et al* 2020 *IOP Conf. Ser.: Mater. Sci. Eng.* **781** 012013

View the [article online](#) for updates and enhancements.

The 17th International Symposium on Solid Oxide Fuel Cells (SOFC-XVII)
DIGITAL MEETING • July 18-23, 2021

EXTENDED Abstract Submission Deadline: February 19, 2021



SUBMIT NOW →

Influence of Deposited Material Energy on Superconducting Properties of the WSi Films

D D Vasilev¹, E I Malevannaya¹, K M Moiseev¹, P I Zolotov^{2,3}, A V Antipov^{2,3}, Y B Vakhtomin^{2,3} and K V Smirnov^{2,3,4}

¹Bauman Moscow State Technical University, 105005, Moscow, Russia

²Moscow Pedagogical State University, 119991, Moscow, Russia

³LLC Superconducting nanotechnology (Scontel), 119021, Moscow, Russia

⁴National Research University Higher School of Economics, 101000, Moscow, Russia

E-mail: d.d.vasilev@bmstu.ru, k.moiseev@bmstu.ru

Abstract. WSi thin films have the advantages for creating SNSPDs with a large active area or array of detectors on a single substrate due to the amorphous structure. The superconducting properties of ultrathin WSi films substantially depends on their structure and thickness as the NbN films. Scientific groups investigating WSi films mainly focused only on changes of their thickness and the ratio of the components on the substrate at room temperature. This paper presents experiments to determine the effect of the bias potential on the substrate, the temperature of the substrate, and the peak power of pulsed magnetron sputtering, which is the equivalent of ionization, a tungsten target, on the surface resistance and superconducting properties of the WSi ultrathin films. The negative effect of the substrate temperature and the positive effect of the bias potential and the ionization coefficient (peak current) allow one to choose the best WSi films formation mode for SNSPD: substrate temperature 297 K, bias potential -60 V, and peak current 3.5 A.

1. Introduction

Superconducting single photon nanowire detector (SNSPD) was developed in 2001 [1]. Such detectors are used as a single photon counter for secure quantum keys' distribution in quantum cryptography [2], in optical space communications [3], for CMOS microcircuit testing [4], visualizing the depth of a subject with high resolution over long distances [5], creating a short-wave infrared single-photon camera [6] etc. To introduce radiation into the meander, a single-mode optical fiber is used, the core thickness of which varies from 9 to 11 μm , so the active region of the meander was initially from 10 to 11 μm , while now it has increased to 14-16 μm to reduce radiation losses [7-11]. If there is an airspace between the photon source and the detector, then it is more efficient to use multimode optical fiber, for example, for use in singlet oxygen luminescence dosimetry (SOLD) [12]. The core diameter of a multimode optical fiber starts at 50 μm , which requires the use of detectors with an active region of about 35 μm in diameter and focusing lenses [13], or detectors with an active region of about 50 μm [14]. Using a matrix of detectors will increase the image parameters of cameras based on single-photon detectors [15]. The demonstrated possibilities of integrating the detector into photonic [16] and plasmonic [17] schemes require the creation of a detectors' array on one substrate with high output parameters [18].



Initially, the detector sensitive element, the meander, was formed on the basis of ultrathin polycrystalline NbN films [19]. Due to the structure and properties of such films are extremely sensitive to the substrate material and the formation conditions, as a result up to now it has not been possible to reproducibly form NbN films on relatively large areas of the substrate. Detectors based on amorphous films, such as WSi [20], MoSi [21], and MoGe [22], are more promising due to their significantly less dependent on the substrate material and its surface structure, as well as less critical to defects in the film itself [23]. Detectors based on amorphous WSi films show high quantum efficiency up to 93% at a telecommunication wavelength of 1550 nm [24]. In addition, due to the smaller band gap and structural homogeneity, detectors based on WSi films with an amorphous structure can effectively register mid-infrared photons with a standard nanowire width of about 100 nm [20], while for detecting mid-infrared photons by means of detectors based on NbN films it is required to decrease the width of the nanowire up to 30 nm, which complicates the manufacturing process [25].

The parameters of the ready-made detector depend on the properties of the ultrathin film of the sensitive element, which in turn depend on its structure. WSi films transfer to the superconducting state at a temperature of about 5 K, the amorphous structure and silicon content of 25% [26]. In this case, the scientific groups during the development of the technology for the formation of WSi films vary the ratio of the components and the film thickness, depositing onto the substrate at room temperature [20, 27-30]. It was noted that WSi films have a lower critical current on MgO substrates in comparison with SiO_x and Si, while the temperature of the transition to the superconducting state on these substrates coincides [30]. An analysis of X-ray diffraction (XRD) showed a non-intense and wide peak of the WSi_2 (110) and W_5Si_3 (202) gratings. Measurements of the film resistance upon application of a magnetic field indicate the anisotropic properties of thin WSi films that are not characteristic of the amorphous structure, which may indicate the presence of a preferred orientation in WSi films [30]. For NbN films, studies were carried out on the effect of the bias potential on the substrate [31], the temperature of the substrate in the region of 825°C [32] and room temperature [33], ion stimulation [34] on the structure and superconducting properties, while the data of the deposited material energy effect on the structure and properties of WSi films are absent. In this paper, we present the results of a study of the magnetron sputtering process technological regimes influence on the superconducting properties of the WSi films.

2. Experiment description

According to the zone model of the film structure for an unbalanced magnetron system, the film structure from zone 1, which is characterized by cone-shaped crystallites separated by voids, transfers to zone 2 (close-packed columnar grains) and 3 (recrystallized grains) with an increase in the substrate temperature, the bias potential on the substrate, and the flux of ions incident on the substrate with respect to the flux of condensing atoms on the substrate (Figure 1) [35]. A study of the influence of all three factors was implemented at the VUP-11M vacuum system at BMSTU, upgraded for WSi films forming process from two magnetron sputtering sources [36]. In our experiment, the substrate temperatures T_s are 297, 447, and 597 K, and the bias potential U_{bias} is 0, -30, -60 V. During the formation of WSi films, silicon is sputtered in the high-frequency mode; therefore, it is possible to control only the ionization of W sputtered in the pulsed mode. The degree of W ionization correlates with the peak current in the pulse I_{peak} , the values of which are 0.5, 2.0, and 3.5 A, based on previous studies [37].

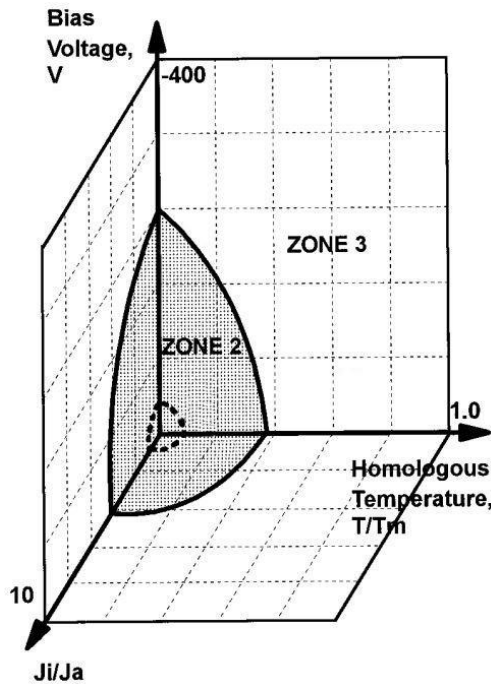


Figure 1. A zone model of the film structure for an unbalanced magnetron system [35].

Influence evaluation of each factor separately and their interaction was carried out according to the full factorial experiment method (Figure 2). To estimate the influence of each factor individually, three additional experiments are carried out at points with a middle value of the varied factors. The experiments are carried out at a working pressure of $2.1 \cdot 10^{-3}$ mbar, an Ar flow of 2.6 l/h, a deposition time of 15 s, a concentration of W of 76%, a specific weight of the film of $8.966 \cdot 10^{-5}$ kg/m², which, according to estimates, corresponds to a thickness of 6 nm.

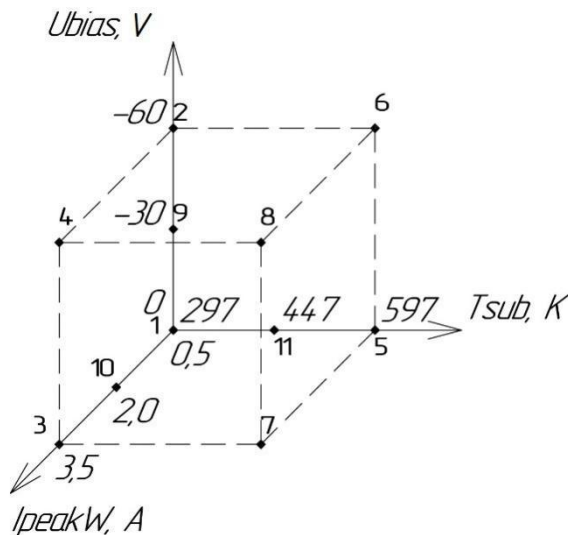


Figure 2. Full factorial experiment scheme.

It should be noted that at film thicknesses less than 10 nm, the thickness value significantly affects their surface resistance and superconducting properties [30]. Due to the influence of the studied factors on the structure, and, consequently, on the density of the formed films, which will change the thickness of the films at the same deposition rate, it was proposed to form films with the same specific weight, which is controlled by the piezoelectric microweighting method according to the previously developed technique [38].

The surface resistance R_s was measured for the obtained WSi films by the four-probe method, and the superconducting properties when the sample was lowered into the pumped-out insert in the cryostat were as follows: critical temperature T_c , transition width ΔT_c , and residual-resistance ratio RRR .

3. Results and discussion

The surface resistance R_s of the WSi films increases with increasing substrate temperature T_s and the bias potential U_{bias} . Peak current I_{peak} does not affect surface resistance (Figure 3).

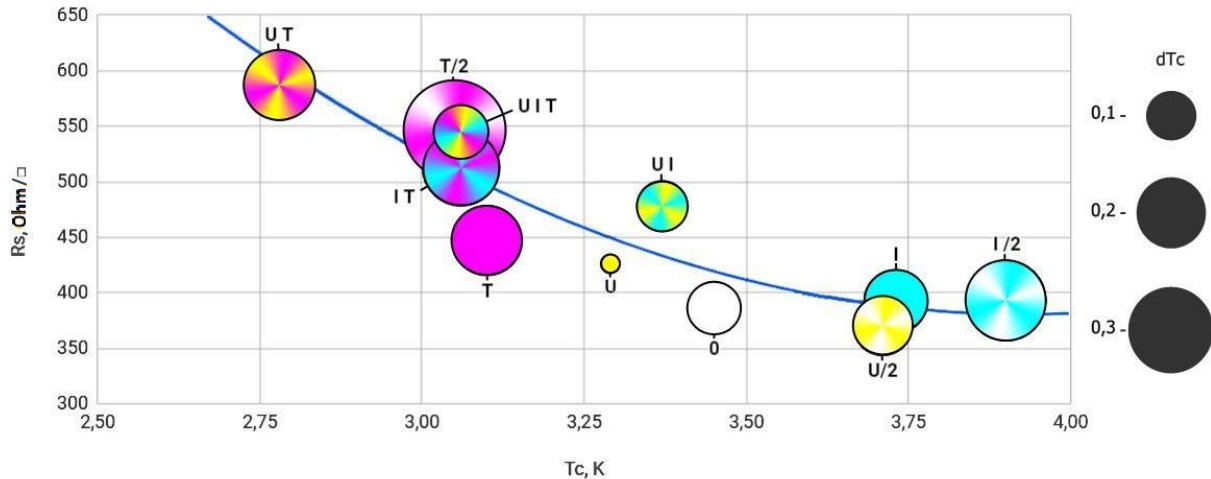


Figure 3. The dependence of surface resistance on the transition temperature of the film, the size is the width of the transition.

The transition temperature T_c decreases with increasing substrate temperature T_s and the bias potential U_{bias} , and increases with increasing peak current I_{peak} .

Variable factors do not affect the residual-resistance ratio RRR (table 1). The dependence of the width of the transition to the superconducting state dT_c on varied factors was also not detected (Figure 3).

Table 1. Surface resistance and superconducting properties of samples.

Sample No	Factors	R_s (Ohm/ \square)	T_c (K)	dT_c (K)	RRR
1	–	387	3.45	0.12	0.95
2	U	426	3.29	0.07	0.96
3	I	392	3.73	0.17	0.94
4	U I	478	3.37	0.12	0.96
5	T	447	3.10	0.20	0.96
6	U T	587	2.78	0.20	0.96
7	I T	513	3.06	0.24	0.95
8	U I T	545	3.06	0.13	0.96
9	U/2	370	3.71	0.15	0.96
10	I/2	393	3.90	0.26	0.95
11	T/2	546	3.05	0.38	0.95

As a result, an increase in the temperature of the substrate increases the surface resistance of the film and decreases the critical temperature, which may be associated with the formation of undesirable bonds between particles of the deposited material and elements of the residual atmosphere or substrate material.

An increase in the bias potential increases the surface resistance without changing the superconducting properties of the film, which can improve the detector signal-to-noise ratio.

An increase in the peak current during W sputtering increases the critical temperature without changing the surface resistance, and can lead to an increase in the critical current density, which can have a positive effect on the detector parameters: signal-to-noise ratio and pulse generation efficiency.

The residual-resistance ratio RRR of the WSi films, unlike NbN, varies from 0.94 to 0.96, which does not allow us to consider this parameter as a tool to improve the output characteristics of the detector.

4. Conclusions

The formation of the WSi films at a substrate temperature of 297 K, a bias potential of -60 V, and a peak current of W 3.5 A complexly increases the surface resistance of the films R_s and the critical transition temperature to the superconducting state T_c , which can positively affect the improvement of the detector signal-to-noise ratio, and contribute to the improvement of the impulse generation of the films. However, to fully estimate the influence of factors on the detector parameters, it is necessary to study the influence of factors on the critical current density and the detector output parameters.

5. Acknowledgment

The research is supported by the Russian Science Foundation project No. 18-12-00364.

References

- [1] Gol'tsman G, Okunev O, Chulkova G, Lipatov A, Semenov A, Smirnov K, Voronov B, Dzardanov A, Williams C and Sobolewski R 2001 *Appl. Phys. Lett.* **79**, 705
- [2] Hoi-Kwong L, Curty M and Tamaki K 2014 *Nat. Photonics* **8**, 595–604
- [3] M. Grein, E. Dauler, A. Kerman, M. Willis, B. Romkey, B. Robinson, D. Murphy, and D. Boroson, "A superconducting photoncounting receiver for optical communication from the Moon," SPIE, 2015
- [4] Zhang J, Boiadjieva N, Chulkova G, Deslandes H, Gol'tsman G, Korneev A, Kouminov P 2003 *Electronics Letters* **39**(14) 1086
- [5] Aongus McCarthy, Nils J. Krichel, Nathan R. Gemmell, Ximing Ren, Michael G. Tanner, Sander N. Dorenbos, Val Zwiller, Robert H. Hadfield and Gerald S. Buller 2013 *Opt. Express* **21**, 8904
- [6] Thomas Gerrits, Daniel J. Lum, Varun Verma, John Howell, Richard P. Mirin, and Sae Woo Nam 2018 *Opt. Express* **26**, 15519
- [7] Iman Esmaeil Zadeh, Johannes W. N. Los, Ronan B. M. Gourgues, Violette Steinmetz, Gabriele Bulgarini, Sergiy M. Dobrovolskiy, Val Zwiller, and Sander N. Dorenbos 2017 *APL Photonics* **2**, 111301
- [8] Lixing You, Jia Quan, Yong Wang, Yuexue Ma, Xiaoyan Yang, Yanjie Liu, Hao Li, Jianguo Li, Juan Wang, Jingtao Liang, Zhen Wang, and Xiaoming Xie 2018 *Opt. Express* **26**, 3 2965
- [9] Li Chen, Dirk Schwarzer, Jascha A. Lau, Varun B. Verma, Martin J. Stevens, Francesco Marsili, Richard P. Mirin, Sae Woo Nam, and Alec M. Wodtke 2018 *Opt. Express* **26**, 12 14859
- [10] Francesco Bellei, Alyssa P. Cartwright, Adam N. McCaughan, Andrew E. Dane, Faraz Najafi, Qingyuan Zhao, and Karl K. Berggren 2016 *Opt. Express* **24**, 4 3248
- [11] P. Zolotov, A. Divochiy, Yu. Vakhtomin, M. Moshkova, P. Morozov, V. Seleznev, and K. Smirnov 2018 *AIP Conference Proceedings* **1936**, 020019
- [12] Nathan R. Gemmell, Aongus McCarthy, Michele M. Kim, Israel Veilleux, Timothy C. Zhu, Gerald S. Buller, Brian C. Wilson, and Robert H. Hadfield 2017 *J. Biophotonics* **10**, 2, 320
- [13] Dengkuan Liu, Shigehito Miki, Taro Yamashita, Lixing You, Zhen Wang, and Hirotaka Terai 2014 *Opt. Express* **22**, 18, 21167
- [14] Hao Li, Lu Zhang, Lixing You, Xiaoyan Yang, Weijun Zhang, Xiaoyu Liu, Sijing Chen, Zhen Wang, and Xiaoming Xie 2015 *Opt. Express* **23**, 13, 17301

- [15] T. Gerrits, S. Allman, D. J. Lum, V. Verma, J. Howell, R. Mirin, and S. W. Nam, "Progress toward a high-resolution single-photon camera based on superconducting single photon detector arrays and compressive sensing," in CLEO: 2015, OSA Technical Digest (online) (Optical Society of America, 2015), paper STh3O.6
- [16] F. Lenzini, N. Gruhler, N. Walter, W. H. P. Pernice 2018 *Adv. Quantum Technol.* **1**, 1800061
- [17] Reinier W. Heeres, Leo P. Kouwenhoven & Valery Zwiller 2013 *Nat. Nanotechnology* **8**, 719
- [18] M. S. Allman, V. B. Verma, M. Stevens, T. Gerrits, R. D. Horansky, A. E Lita, F. Marsili, A. D. Beyer, M. D. Shaw, D. Kumor, R. Mirin, and S. W. Nam 2015 Proc. SPIE 9504, *Photon Counting Applications* 2015, 950402
- [19] J. R. Gao and M. Hajenius 2007 *Appl. Phys. Lett.* **91**, 062504
- [20] Burm Baek, Adriana E. Lita, Varun Verma, and Sae Woo Nam 2011 *Appl. Phys. Lett.* **98**, 251105
- [21] Korneeva Y P, Mikhailov M Y, Pershin Y P, Manova N N, Divochiy A V, Vakhtomin Y B, and Goltsman G N 2014 *Superconductor Science and Technology* **27**, 095012
- [22] V. B. Verma, A. E. Lita, M. R. Vissers, F. Marsili, D. P. Pappas, R. P. Mirin, and S. W. Nam 2014 *Appl. Phys. Lett.* **105**, 022602
- [23] Lita, A., Verma, V., Horansky, R., Shainline, J., Mirin, R., & Nam, S. (2015). Materials Development for High Efficiency Superconducting Nanowire Single-Photon Detectors. MRS Proceedings, 1807, 1-6
- [24] Marsili F, Verma V B, Stern J A, Harrington S, Lita A E, Gerrits T and Nam S W 2013 *Nature Photonics* **7**(3) 210
- [25] Francesco Marsili, Francesco Bellei, Faraz Najafi, Andrew E. Dane, Eric A. Dauler, Richard J. Molnar, Karl K. Berggren 2012 *Nano Lett.* 20121294799-4804
- [26] Kondo S 1992 *Journal of materials research* **7**(04), 853
- [27] X. Zhang, A. Engel, Q. Wang, A. Schilling, A. Semenov, M. Sidorova, H.-W. Hübers, I. Charaev, K. Ilin, and M. Siegel 2016 *Phys. Rev. B* **94**, 174509
- [28] V A Seleznev, A V Divochiy, Yu B Vakhtomin, P V Morozov, P I Zolotov, D D Vasil'ev, K M Moiseev, E I Malevannaya and K V Smirnov 2016 *J. Phys.: Conf. Ser.* **737** 012032
- [29] I. N. Florya, Yu. P. Korneeva, M. Yu. Mikhailov, A. Yu. Devizenko, A. A. Korneev, and G. N. Goltsman 2018 *Low Temperature Physics* **44**, 221
- [30] Jin Jin, Fengfeng Fu, Xiaoqing Jia, Lin Kang, Zhihe Wang, Xuecou Tu, Labao Zhang 2019 *IEEE Transactions on Applied Superconductivity* **29**, 5, 18483128
- [31] Andrew E. Dane, Adam N. McCaughan, Di Zhu, Qingyuan Zhao, Chung-Soo Kim, Niccolo Calandri, Akshay, Agarwal, Francesco Bellei, and Karl K. Berggren 2017 *Appl. Phys. Lett.* **111**, 12260
- [32] K Ilin et al 2008 *J. Phys.: Conf. Ser.* **97** 012045
- [33] Zhen Wang, Akira Kawakami, Yoshinori Uzawa, and Bokuji Komiyama 1996 *J Appl. Phys.* **79**, 7837
- [34] Tomas Polakovic, Sergi Lendinez, John E. Pearson, Axel Hoffmann, Volodymyr Yefremenko, Clarence L. Chang, Whitney Armstrong, Kawtar Hafidi, Goran Karapetrov, and Valentine Novosad 2018 *APL Materials* **6**, 076107
- [35] P. J. Kelly and R. D. Arnell 1998 *Journal of Vacuum Science & Technology A* **16**, 2858
- [36] D D Vasilev et al 2017 *J. Phys.: Conf. Ser.* **872** 012027
- [37] Akishin M Y, Malevannaya E I, Vasiliev D D and Moiseev K M 2017 *Materials of the 24th Scientific and Technical Conf. with the participation of foreign specialists "Vacuum science and technology"* ed S B Nesterov (Moscow: NOVELLA) 193-6 (in Russian)
- [38] Vasiliev D D, Malevannaya E I and Moiseev K M 2018 *25th Scientific and Technical Conf. with the participation of foreign experts "Vacuum Science and Technology"* ed S B Nesterov (Moscow: NOVELLA) 221-7 (in Russian)